ELSEVIER

Biophysical Chemistry 127 (2007) 103–112

Biophysical Chemistry

http://www.elsevier.com/locate/biophyschem

A molten globule-like intermediate state detected in the thermal transition of cytochrome *c* under low salt concentration ☆

Shigeyoshi Nakamura [a], Takayuki Baba [a], Shun-ichi Kidokoro [a,b,*]

[a] *Department of Bioengineering, Nagaoka University of Technology, 1603-1 Kamitomioka, Nagaoka 940-2188, Japan*
[b] *Genome Science Center, Riken, 1-7-22 Suehiro-cho, Tsurumi-ku, Yokohama 230-0045, Japan*

Received 25 November 2006; received in revised form 3 January 2007; accepted 4 January 2007
Available online 12 January 2007

Abstract

To understand the stabilization mechanism of the transient intermediate state in protein folding, it is very important to understand the structure and stability of the molten globule state under a native condition, in which the native state exists stably. The thermal transitions of horse cytochrome *c* were thermodynamically evaluated by highly precise differential scanning calorimetry (DSC) at pH 3.8–5.0. The heat capacity functions were analyzed using double deconvolution and the nonlinear least-squares method. An intermediate (I) state is clearly confirmed in the thermal native (N)-to-denatured (D) transition of horse cytochrome *c*. The mole fraction of the intermediate state shows the largest value, 0.4, at nearly 70 °C at pH 4.1. This intermediate state was also detected by the circular dichroism (CD) method and was found to have the properties of the molten globule-like structure by three-state analysis of the CD data. The Gibbs free-energy change between N and I, ΔG_{NI}, and that between N and D, ΔG_{ND}, were evaluated to be 9–22 kJ mol^{-1} and 41–45 kJ mol^{-1}, respectively at 15 °C and pH 4.1.

Keywords: Molten globule; Cytochrome *c*; Differential scanning calorimetry; Circular dichroism; Thermal transition; Gibbs free energy change

1. Introduction

Many globular proteins have been known to exhibit an equilibrium molten globule (MG) state, which is a compact denatured state with a native-like secondary structure but a largely disordered tertiary structure [1–3]. It was reported that the equilibrium MG state of each protein is identical to its transient intermediate on folding [2,4–6]. However, most equilibrium MG states are stabilized under special solution conditions, such as low pH and high anion concentration. The transient intermediate state in protein folding is observed under a native condition, in which the native state exists stably. The stability of the equilibrium MG state in a native condition is very important for understanding the stabilization mechanism of the transient intermediate state in protein folding.

Cytochrome *c* is a small globular protein of 104 residues with a heme region [7]. Its equilibrium intermediate state was one of the first examples of the MG state [1]. The equilibrium MG states of cytochrome *c* were reported under special solution conditions, such as low pH and a high concentration of anions [1,8,9]; a low concentration of denaturant, alcohol, or surfactant [10–15]; and acetylation of the side chain of lysine residues at low pH [16]. The MG state of the mutant yeast cytochrome *c* by site-directed mutagenesis to rupture the hydrogen bond of two omega loops was observed at neutral pH [17].

The structural characteristics of the MG state of cytochrome *c* show that the native-like secondary structure is retained; that most of the specific tertiary structure of the native state, such as the rigid side-chain packing, is absent; and that the molecules are globular and compact [1,2,18]. The stability of the MG state of cytochrome *c* at low pH and with a high concentration of anions was studied in the transition from the MG to the D state [19–21] and the transition from the N to the MG state [22]. The pH-induced transition from the N to the MG state of bovine cytochrome *c* was well explained with the two-state transition

☆ This work was supported by Grants-in-Aids from the Ministry of Education, Culture, Sports, Science, and Technology (MEXT) of Japan. S.N. was supported by a fellowship from the Japan Society for the Promotion of Science to Young Scientists.

* Corresponding author. Department of Bioengineering, Nagaoka University of Technology, 1603-1 Kamitomioka, Nagaoka 940-2188, Japan. Tel./fax: +81 258 47 9425.
E-mail address: kidokoro@nagaokaut.ac.jp (S. Kidokoro).

0301-4622/$ - see front matter © 2007 Elsevier B.V. All rights reserved.
doi:10.1016/j.bpc.2007.01.002

model by isothermal acid-titration calorimetry (IATC) [22]. Although the MG-to-D-state transition of horse cytochrome *c* was well explained by the two-state transition model using differential scanning calorimetry (DSC) and isothermal titration calorimetry (ITC) [19,21], it was reported that the intermediate state exists in the thermal transition from the MG to the D state by a circular dichroism (CD) study [20].

The stability of the MG state at low pH and high anion concentration was suggested to be determined by a balance of electrostatic repulsions between positive residues, which favor the extended conformation, and the opposing forces such as hydrophobic interaction, which stabilize the MG state [16]. However, the stability of the equilibrium MG state of cytochrome *c* under a native condition has not been examined in detail.

Here it is worthwhile to be reminded that our fundamental knowledge of the thermodynamic mechanism to determine the stability of small globular proteins has been revealed by differential scanning calorimetry (DSC) [23–25]. Those studies showed that the thermal transition of these proteins–bovine cytochrome *c*, metmyoglobin, α-chymotrypsin, and myoglobin–could be well explained by the two-state transition model as the first approximation, judging from the coincidence between the directly observed calorimetric enthalpy (ΔH^{cal}) and the van't Hoff enthalpy (ΔH^{vH}) evaluated by assuming the two-state model. Additionally, the small difference between these two enthalpies also suggested an intermediate state populating around the transition temperature, although the fraction of the intermediate state was too small to be characterized quantitatively in the previous studies. Because of the recent development of DSC method, it is highly expected to examine these equilibrium intermediate states in the thermal transition in order to clarify the relationship between the intermediate state and the MG state under a native condition.

In this study, we have confirmed the existence of an intermediate state in the thermal transition of horse cytochrome *c* under a low salt concentration at around pH 4 by using a highly precise differential scanning calorimeter, VP-DSC. In addition, we have detected a molten globule-like intermediate state of cytochrome *c* spectroscopically. We have also evaluated the thermodynamic parameters of the thermal transition of cytochrome *c*, including the intermediate state.

2. Materials and methods

2.1. Cytochrome c solution

Lyophilized powder of horse cytochrome *c* (c-2506; Sigma, St. Louis, MO, USA) was dissolved in 50 mM sodium acetate/acetic acid buffer at pH 3.8–5.0. This protein solution was dialyzed with a dialysis membrane, Spectra/Por (132660; Spectrum Laboratories, Rancho Dominguez, CA, USA), whose cutoff molecular weight is 6–8 kDa, at 4 °C for about 1 day against 1 l buffer. The protein solution was ultra-filtrated with a MolCut ultra filter unit (USY-20; Advantec, Tokyo, Japan), whose cutoff molecular weight is 0.2 MDa, in order to remove any aggregation that may be produced during the dialysis. The concentration of horse cytochrome *c* was determined with a UB-35 spectrophotometer (Jasco, Tokyo, Japan) using the extinction coefficient of $\varepsilon_{409}=10.6\times10^4\ \mathrm{M^{-1}cm^{-1}}$. Before each experiment, the solution was degassed for several minutes by aspiration with a membrane pump (ULVAC, Kanagawa, Japan) and by sonication simultaneously with the Perl Clean sonication device (Fkk, Tokyo, Japan).

2.2. Differential scanning calorimetry

Differential scanning calorimetry (DSC) experiments of cytochrome *c* were performed with a highly sensitive differential scanning calorimeter, VP-DSC (Microcal, Los Angeles, CA, USA). The experiments were performed using 1.0 mg/ml cytochrome *c* solution at pH 3.8–5.0, 50 mM sodium acetate/acetate buffer. At each pH the transition was reversible, as demonstrated by repeated scans of the same sample. It was confirmed that the heat capacity profiles observed at the scanning rate of 1 K/min and 0.5 K/min agree perfectly at pH 4.1. Thus, the thermal transition process can be considered to be in equilibrium and therefore can be analyzed thermodynamically. Without mentioning in particular, the DSC experiments were done at a scanning rate of 1 K/min. Absolute heat capacity, C_{p}, is determined by the equation [23],

$$C_{\mathrm{p}} = \Delta C_{\mathrm{p}}^{\mathrm{app}} + V_{\mathrm{p}}\frac{C_{\mathrm{s}}}{V_{\mathrm{s}}} \tag{1}$$

where $\Delta C_{\mathrm{p}}^{\mathrm{app}}$ is the apparent heat capacity determined by DSC and V_{p} is the partial volume of cytochrome *c* determined by density measurement using a highly precise vibrating tube densimeter, DMA5000 (Anton Paar, Graz, Austria); 9160± 30 ml $\mathrm{mol^{-1}}$ at pH 4.1. C_{s} and V_{s} are the heat capacity and partial volume of the solvent, respectively.

The heat capacity functions were analyzed by double deconvolution (DD) method, which analyzes the heat capacity functions as reported previously [26,27], and the nonlinear least-squares method with the three-state model. The DD method can determine the enthalpy and the Gibbs free energy directly from the heat capacity function of the native (N), denatured (D), and intermediate (I) states of these states in the transition, using the following Eqs. (2)–(6).

The observed enthalpy, $H^{\mathrm{obs}}(T)$, and the observed Gibbs free energy, $G^{\mathrm{obs}}(T)$, were directly deduced from observed heat capacity functions (C^{obs}) using Eqs. (2) and (3). Also, the enthalpy of the native and denatured states, $H_{\mathrm{N}}(T)$ and $H_{\mathrm{D}}(T)$, was directly evaluated from the heat capacity functions of the native state (C_{N}) and the denatured state (C_{D}) using Eq. (2). The Gibbs free energy of the native and the denatured states, $G_{\mathrm{N}}(T)$ and $G_{\mathrm{D}}(T)$, were also directly calculated from the heat capacity functions of the native and denatured states using Eq. (3). C_{N} and C_{D} were evaluated by linear least-squares fitting of heat capacity in the pre- and post-transition temperature ranges, respectively.

$$H = \int_{T_0}^{T} C_{\mathrm{p}}\mathrm{d}T \tag{2}$$

$$G = -T\int_{T_0}^{T}\frac{H}{T^2}\mathrm{d}T. \quad (3)$$

The mole fractions of the native and the denatured states, were determined by Eq. (4).

$$f_i(T) = \exp\left[-\frac{G_i(T)-G^{\mathrm{obs}}(T)}{RT}\right] \quad (4)$$

where f_i and G_i shows the mole fraction and Gibbs free energy of each state, native (N) and denatured (D) states.

When an intermediate state exists in thermal transition, the mole fraction of the intermediate state, f_{I}, is determined with Eq. (5).

$$f_{\mathrm{I}}(T) = 1-f_{\mathrm{N}}(T)-f_{\mathrm{D}}(T) \quad (5)$$

The enthalpy of the intermediate state, $H_{\mathrm{I}}(T)$, was determined from Eq. (6) [26,27].

$$H_{\mathrm{I}}(T) = \frac{H^{\mathrm{obs}}(T)-f_{\mathrm{N}}(T)H_{\mathrm{N}}(T)-f_{\mathrm{D}}(T)H_{\mathrm{D}}(T)}{f_{\mathrm{I}}(T)} \quad (6)$$

The van't Hoff enthalpy was calculated with Eq. (7) [26,27].

$$\Delta H_{\mathrm{ND}}^{\mathrm{vH}}(T) = RT^2\left\{\frac{\Delta C_{\mathrm{N}}}{\Delta H_{\mathrm{N}}}-\frac{\Delta C_{\mathrm{D}}}{\Delta H_{\mathrm{D}}}\right\} \quad (7)$$

where ΔC_{N}, ΔC_{D}, ΔH_{N}, and ΔH_{D} were defined by the following equations.

$$\Delta C_i = C^{\mathrm{obs}}-C_i \quad (8)$$

$$\Delta H_i = H^{\mathrm{obs}}-H_i \quad (9)$$

where ΔC_i, C_i, ΔH_i, and H_i, show ΔC, C, ΔH, and H, of each state, N and D states, respectively.

The thermodynamic parameters determined by the DD method were refined by the nonlinear least-squares fitting method [26,27] using SALS software [28]. The fitting of the heat capacity functions by the three-state transition model was carried out with several fitting parameters: enthalpy change, ΔH, heat capacity change, ΔC_{p}, and mid-point temperature, T_{m}, of the thermal transitions (the transition from the N to the I states and that from the N to the D states). In this nonlinear least-squares fitting with the three-state model, the heat capacity change of the transition from the N to the I states, $\Delta C_{\mathrm{p,\,NI}}$, was fixed to zero in order to suppress the degrees of freedom of the fitting. Because the $\Delta C_{\mathrm{p,\,ND}}$ determined by the three-state analysis has a rather large error (see Table 1), the $\Delta C_{\mathrm{p,\,ND}}$ was evaluated from the temperature dependence of the enthalpy change of the transition from the N to D states at the transition temperature, ΔH_{ND}, assuming that the pH dependence of the enthalpy change, $\left(\frac{\partial \Delta H}{\partial pH}\right)$, is zero. It was reported that $\Delta C_{\mathrm{p,\,ND}}$ was not influenced so much in $\left(\frac{\partial \Delta H}{\partial pH}\right)$ [29]. On the other hand, the $\left(\frac{\partial \Delta H}{\partial pH}\right)$ in the transition from the N to the MG state of bovine cytochrome *c* cannot be disregarded [22].

2.3. Isothermal acid-titration calorimetry

Isothermal acid-titration calorimetry (IATC) is a method for evaluating the enthalpy of protein molecules as a function of pH using isothermal titration calorimetry (ITC) and pH measurement [22,29]. The experiments were performed with 0.5 mg/ml cytochrome *c* solution of 20 mM KCl. The HCl titration was measured with an isothermal titration calorimeter, the ITC unit of MCS (MicroCal, Northampton, MA, USA) with a cell volume of 1.368 ml. The titration was carried out with injections of 2, 5, and 10 μl of 20–400-mM HCl solution in 20 mM KCl by using a 250 μl syringe. A control experiment was performed with the reference solution, 20 mM KCl solution. The pH of the HCl titration was measured by using a glass electrode and a pH meter, F23 (Horiba, Kyoto, Japan). The solution used for the pH measurements was identical to that used for the calorimetric measurements. For the pH measurements, the initial volume of the protein solution was 10 ml, and the injection volumes were determined as the ratios between the initial and injection volumes became identical to those of each corresponding injection in the ITC measurements. The temperature of the titration vessel for pH measurement was kept constant in a handmade glass bath with circulating water from a thermostat water bath, VM-150 (Advantec, Tokyo, Japan). The dilution heat of HCl solution was corrected as previously described [29]. The neutralization heat was observed above pH 4. The pH dependence of the neutralization heat was estimated by the

Table 1
The thermodynamic parameters, such as the mid-point temperature, T_{m}, the enthalpy change, ΔH, and the heat capacity change, ΔC_{p} on the thermal transition of horse cytochrome *c* determined by DSC and IATC

pH	$T_{\mathrm{m,NI}}$/°C	ΔH_{NI}/kJ mol^{-1}	$T_{\mathrm{m,ND}}$/°C	ΔH_{ND}/kJ mol^{-1}	$\Delta C_{\mathrm{p,ND}}$[a]/kJ K^{-1} mol^{-1}	$\Delta C_{\mathrm{p,ND}}$[b]/kJ K^{-1} mol^{-1}	$\Delta H_{\mathrm{ND}}-2$[c]/kJ mol^{-1}
3.8	68±2	141±8	68.0±0.3	449±6	57±0.7		378±2
4.1	69±1	141±6	70.2±0.3	468±6	5.6±0.7	6.2±0.1	391±2
4.5	73±1	155±6	74.1±0.2	498±6	6.3±0.7		413±1
5.0	73±1	157±3	762±0.2	520±4	5.8±0.7		422±1
2.9[d]			40[d]	288±1[d]			

The ΔH was evaluated at T_{m}.
[a] These values of the ΔC_{p} were determined by the three-state analysis of the heat capacity function.
[b] This value of the ΔC_{p} was the linear fitting of the temperature dependence of ΔH (see Fig. 5).
[c] These values of the ΔH were determined by the two-state analysis.
[d] These data were evaluated by IATC method.

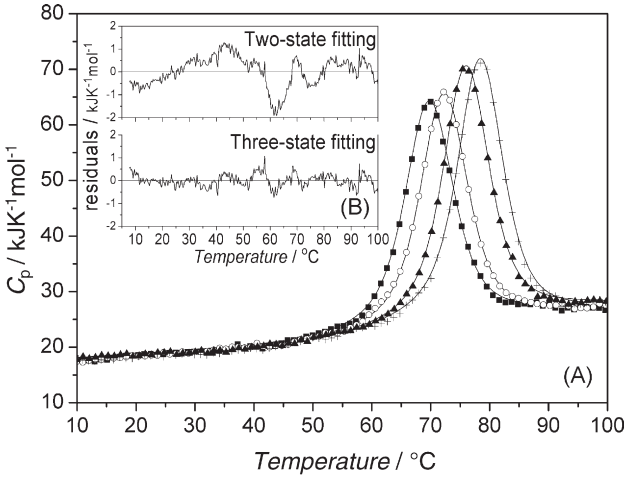

Fig. 1. (A) The temperature dependence of the partial molar heat capacity of horse cytochrome *c* at pH 3.8 (closed squares), 4.1 (open circles), 4.5 (closed triangles), and 5.0 (crosses). The solid lines show the theoretical fitting curves determined by the analysis with the three-state transition model. (B) The residuals of two-state (upper graph) and three-state (lower graph) fittings.

quadratic fitting of the heat from reference experiments at this pH range, and the neutralization heat was corrected from the heat of sample experiments. In this study, the neutralization heat is very small compared with the heat from the pH-induced structure transition of cytochrome *c*. The enthalpy function of pH was analyzed with a two-state model and the nonlinear least-squares fitting process by Eqs. (10)–(12) as previously described [22,29].

$$H(\mathrm{pH}) = H_{\mathrm{N}}(\mathrm{pH})[1-f_{\mathrm{D}}(\mathrm{pH})] + H_{\mathrm{D}}(\mathrm{pH})f_{\mathrm{D}}(\mathrm{pH}), \tag{10}$$

where H_{N} and H_{D} are the enthalpy functions of the native and acid-denatured states, respectively, and $f_{\mathrm{D}}(\mathrm{pH})$ is the molar fraction of the denatured state.

$$f_{\mathrm{D}}(\mathrm{pH}) = \{1 + \exp[\Delta G(\mathrm{pH})/RT]\}^{-1} \tag{11}$$

where $\Delta G(\mathrm{pH})$ is the Gibbs free-energy change, and R and T are the gas constant and temperature, respectively.

$$\Delta G(\mathrm{pH}) = (\ln 10)RT \int_{pH_{\mathrm{d}}}^{\mathrm{pH}} \Delta v(\mathrm{pH})\mathrm{d}pH \tag{12}$$

where $\Delta v(\mathrm{pH})$ is the proton-binding number difference, and $\mathrm{pH_d}$ is the mid-point in the pH transition of the protein molecule. The enthalpy functions of the native and acid-denatured states were approximated as constants in this study.

2.4. Circular dichroism spectroscopy

Circular dichroism (CD) spectra in the far-UV (215–250 nm), the near-UV (270–330 nm), and the soret (390–440 nm) regions of cytochrome *c* were measured with a spectropolarimeter, J-720 (Jasco, Tokyo, Japan) with 1-cm path-length quartz cells in the temperature range of 20–95 °C. The experiments were performed with 0.07–0.45 mg/ml cytochrome *c* in 50 mM sodium acetate/acetic acid buffer at pH 4.1. The cell temperature was controlled with a temperature control unit, PTC-343W (Jasco). The temperature dependences of the molar ellipticity, $[\theta]$, at 222 nm, 282 nm, 289 nm, and 416 nm were measured at 20 °C–95 °C. The scanning rate of heating was 1 °C/min. The normalized CD ($[\theta]^{\mathrm{nor}}$) was calculated by the following.

$$[\theta]^{\mathrm{nor}}(T) = \frac{[\theta](T)-[\theta]_{\mathrm{N}}(T)}{[\theta]_{\mathrm{D}}(T)-[\theta]_{\mathrm{N}}(T)} \tag{13}$$

where $[\theta]_{\mathrm{N}}$ and $[\theta]_{\mathrm{N}}$ represent the molar ellipticity of the native and denatured states determined from the baselines of the pre- and post-transition, respectively, determined by linear least-squares fitting (Eq. (14)) in the temperature range of 20–30 °C

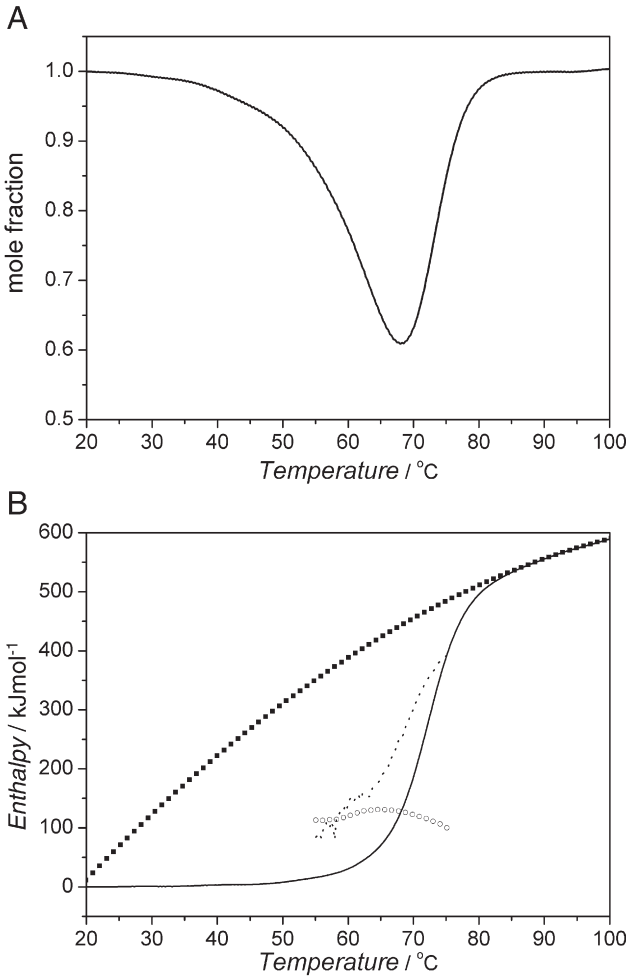

Fig. 2. (A) The sum of the mole fraction of the native and denatured states of cytochrome *c* in the thermal transition at pH 4.1 calculated by the double deconvolution (DD) method. (B) The temperature dependence of the enthalpies of cytochrome *c* determined by the DD method. The solid lines show the ΔH_{N}, which is defined as $H^{\mathrm{obs}}-H_{\mathrm{N}}$, where H^{obs} is the observed enthalpy and H_{N} is the enthalpy of the N state of cytochrome *c*. The filled squares show the calorimetric enthalpy, ΔH^{cal}, which is defined as $H_{\mathrm{D}}-H_{\mathrm{N}}$, where H_{D} is the enthalpy of the D state of cytochrome *c*. The open circles show the ΔH_{NI}, which is defined as $H_{\mathrm{I}}-H_{\mathrm{N}}$, where H_{I} is the enthalpy of the intermediate state on thermal N–D transition. The dotted lines show the van't Hoff enthalpy.

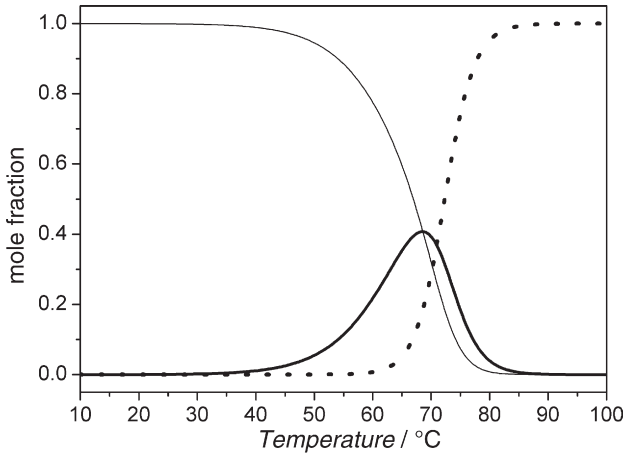

Fig. 3. The temperature dependence of the mole fraction of each state of cytochrome *c* at pH 4.1 determined by the three-state analysis with the nonlinear least squares method. The mole fractions of the native (thin solid line), the intermediate (thick solid line), and the denatured (dotted line) state were shown.

for the native state and in 85–95 °C for the denatured state at all the wavelengths.

$$[\theta]_i = A_i(T-T_0) + B_i \tag{14}$$

where T_0 was fixed to 273.15 K in this analysis. The estimated values for the two fitting parameters, A_i and B_i (i=N, D), were determined for each wavelength as shown here: at 222 nm (A_N; −2, B_N; −9.8, A_D; 5, B_D; −4.9), at 282 nm (A_N; −40, B_N; −6.3, A_D; −30, B_D; 5.5), at 289 nm (A_N; −20, B_N; −8.6, A_D; −20, B_D; 2.0), and at 416 nm (A_N; −10, B_N; −28, A_D; −130, B_D; 63) where A_i is in the unit of deg cm^2 dmol^{-1} K^{-1}, and B_i is in kdeg cm^2 dmol^{-1}.

The normalized CD of the intermediate state ($[\theta]_I^{nor}(T)$) is evaluated by Eq. (15).

$$[\theta]_I^{nor}(T) = \frac{[\theta]^{nor}(T) - f_D(T)}{f_I(T)} \tag{15}$$

The mole fraction functions of each state determined by DSC were used in this analysis.

3. Results

3.1. Thermal transition of cytochrome c evaluated by calorimetry

Fig. 1 shows the temperature dependences of the partial molar heat capacities of cytochrome *c* at pH 3.8, 4.1, 4.5, and 5.0. It was confirmed that these thermal transitions from DSC experiments satisfied to be in equilibrium as mentioned in Materials and methods.

Fig. 2A shows the sum of the mole fraction of the native and denatured states, f_N+f_D, of cytochrome *c* calculated by the DD method. The negative peak was observed at 50–80 °C. The minimum value of the mole fraction of the sum of the native and denatured states is about 0.6 at around 70 °C. This indicates that the mole fraction of the intermediate state is about 0.4 at around 70 °C.

Fig. 2B shows the enthalpy functions of each state of cytochrome *c* on the thermal transition at pH 4.1 as determined by the DD method. The ΔH_N increases sharply from 60 to 80 °C. The van't Hoff enthalpy, ΔH^{vH}, is smaller than ΔH^{cal} throughout this temperature range. The ΔH^{vH} and ΔH^{cal} are 321 kJ mol^{-1} and 459 kJ mol^{-1}, respectively, at the mid-point temperature, T_m, of the N–D transition. $\frac{\Delta H^{vH}}{\Delta H^{cal}}$ is 0.7 at T_m. This strongly indicates the existence of the intermediate state in this transition.

This increase of ΔH_N corresponds to the enthalpy change in the thermal N–D transition of cytochrome *c*. ΔH_{NI} is about 100 kJ mol^{-1} at 60–70 °C.

Based on these results, we analyzed the heat capacity functions of cytochrome *c* by the nonlinear least-squares method using the three-state model. In Fig. 1A, the solid lines show the theoretical fitting curve calculated with the three-state analysis. These theoretical curves agree with the experimental heat capacity data very well. Fig. 1B shows the residuals of two-state and three-state fittings. The residual of two-state fitting is larger than that of three-state fitting, particularly in the pre-transition temperature range. The root mean square deviations of the analysis with the two-state and three-state transition models are 0.40 and 0.18 μW, respectively. The difference in the deviations between the two- and three-state models is significant in comparison with the noise of the calorimeter, VP-DSC: 0.10 μW, as evaluated by DSC measurement of water.

Fig. 3 shows the mole fraction function of temperature in each state–N, I, and D–on the thermal transition of horse cytochrome *c* at pH 4.1 determined by the three-state analysis with the nonlinear least-squares method. The mole fraction of the I state is largest, 0.4, at about 70 °C. The thermodynamic parameters of the N–D thermal transition of horse cytochrome *c* are shown in Table 1. The ΔH_{ND}, determined by using DSC with the three-state analysis, shows values that are about 100 kJ mol^{-1} higher than the value of ΔH_{ND} with two-state analysis.

The thermodynamic parameter at low temperature was evaluated by isothermal acid-titration calorimetry (IATC) to

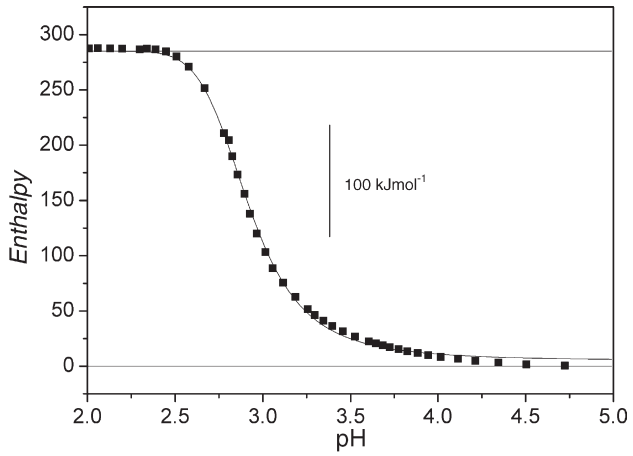

Fig. 4. The enthalpy as a function of pH on acid denaturation of horse cytochrome *c* at 40 °C. The filled squares show the experimental data. The solid lines show the theoretical fitting curve and the base lines of the native and denatured states.

confirm the correctness of these thermodynamic parameters determined by the three-state analysis from DSC experiments. Fig. 4 shows the enthalpy function of pH on the acid-denaturation of horse cytochrome *c* at 40 °C evaluated by IATC. The acid-denaturation of the protein molecule is observed in the pH range 3.5–2.5. The theoretical curves calculated with the two-state transition model agree with the experimental data. The mid-point pH, pH_d, is 2.9 on the pH-induced transition from the N to the D state. The proton binding-number difference, Δv, is 2.9 and the enthalpy change, ΔH, is 288 kJ mol^{-1} in the transition.

Fig. 5 shows the temperature dependence of the ΔH of horse cytochrome *c* determined by DSC and IATC. The values of ΔH_{ND} determined by the present study using DSC with the three-state analysis are higher than the values of ΔH_{ND} previously reported [30] by about 100 kJ mol^{-1}. The value of ΔH_{ND} determined by ITAC is also higher by 100 kJ mol^{-1}. On the other hand, the ΔH_{ND} determined with the two-state model agrees almost completely with the ΔH_{ND} reported previously [30]. The ΔH^{cal} and ΔH^{vH} at T_m determined with the two-state model in pH 4.1 are 393 kJ mol^{-1} and 391 kJ mol^{-1}, and the $\frac{\Delta H^{vH}}{\Delta H^{cal}}$ becomes 1.0.

The heat capacity change, $\Delta C_{p,\ ND}$, is calculated from the temperature dependence of ΔH_{ND} obtained by DSC and IATC using linear least-squares fitting. The $\Delta C_{p,\ ND}$ of horse cytochrome *c* is 6.2 kJ K^{-1}mol^{-1} in this study. This result is identical to $\Delta C_{p,\ ND}$ previously reported [30]. The $\Delta C_{p,\ ND}$ determined by the temperature dependence of ΔH_{ND} and the $\Delta C_{p,\ ND}$ deduced from three-state analysis of the single heat capacity profile agree within error (see Table 1). In this study, the nonlinear least-squares fitting with the three-state model was performed with $\Delta C_{p,\ NI}$ fixed to 0 kJ K^{-1}mol^{-1} in order to reduce the degrees of freedom of the fitting. It was confirmed that these two $\Delta C_{p,\ ND}$, determined by the temperature dependence of ΔH_{ND} and $\Delta C_{p,\ ND}$ deduced from three-state analysis of the single heat capacity profile, agree within error with $\Delta C_{p,\ NI}$ fixed to 0–3 kJ K^{-1}mol^{-1}. In the case where $\Delta C_{p,\ NI}$ is fixed to over 3 kJ K^{-1}mol^{-1}, however, the $\Delta C_{p,\ ND}$ deduced from three-state analysis of the single heat capacity profile was lower than that determined by the temperature dependence of ΔH_{ND}.

It was found that at least one intermediate state exists in the thermal unfolding of cytochrome *c* under not only the low salt condition as shown here but also several salt conditions such as with 0–500 mM KCl and 0–80 mM $NaClO_4$, and that this three-state characterization on the thermal transition is observed in bovine cytochrome *c* (data not shown).

3.2. Thermal transition of cytochrome c evaluated by circular dichroism measurement

CD experiments were performed to confirm the existence of the intermediate state in the thermal transition of cytochrome *c* that was observed by DSC experiments. Fig. 6A shows the CD spectra of far-UV (215–250 nm), near-UV (270–330 nm), and Soret (370–440 nm) regions of horse cytochrome *c* at 20 °C, 70 °C, and 95 °C. The CD spectra at 20 °C show the structure of

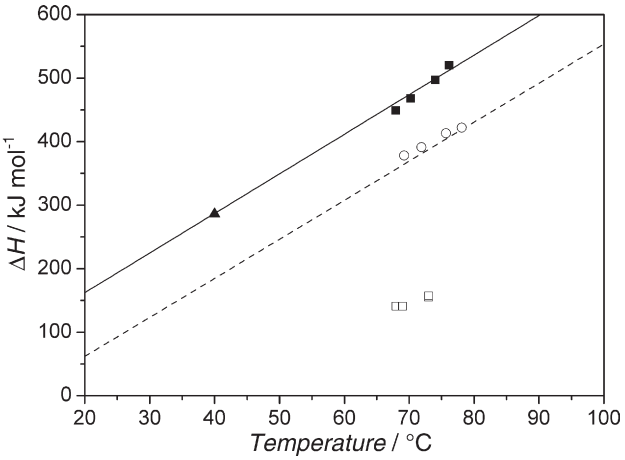

Fig. 5. The temperature dependence of the enthalpy change, ΔH, obtained by DSC and IATC methods. The filled squares show the enthalpy change from the N to the D state, ΔH_{ND}, determined by DSC with the three-state transition model. The open squares show that from the N to the I state, ΔH_{NI}. The open circles show the ΔH_{ND}, determined with the two-state transition model. The filled triangles show the enthalpy change from the N to the D state, ΔH_{ND}, determined by IATC. The solid line represents the fitting line of ΔH_{ND} from DSC and IATC in this study. The broken line shows ΔH_{ND} by the two-state transition analysis reported previously [30].

the N state and those at 95 °C show the structure of the D state (see Fig. 3). At 70 °C, the mole fractions of the N, I, and D states are 0.31, 0.39, and 0.30, respectively, judging from the mole fraction functions from DSC. So the CD spectra at 70 °C show the mixture of the spectra of the N, I, and D states. In far-UV CD, the CD spectrum at 20 °C shows a large negative peak at 222 nm, which derives from the quantity of the alpha-helix structures. This negative peak decreased in the spectrum at 95 °C. The CD spectrum at 70 °C shows a negative peak in the middle of the CD spectra at 20 °C and 95 °C. In near-UV CD, the CD spectra at 20 °C show two negative peaks, at 282 nm and 289 nm, reflecting the tertiary structure change derived from the side-chain packing of tryptophane residue of the protein molecule. These two peaks disappear in the CD spectra at 95 °C. In the soret region, the CD spectrum at 20 °C shows a large negative peak of the Cotton effect at 416 nm, reflecting the interactions between Met 80 and the heme region [31,32]. This negative peak disappears above 70 °C. This indicates that the interactions between Met 80 and the heme region disappear above 70 °C. The temperature dependence of the molar ellipticity, $[\theta]$, on the thermal transition of cytochrome *c* is evaluated at several wavelengths, which probe different types of structure information.

Fig. 6B shows the temperature dependence of the normalized CD of several wavelengths–222, 282, 289, and 416 nm–on the thermal transition of horse cytochrome *c* at pH 4.1. The normalized CDs are deduced as described in Materials and methods. The normalized CDs at 222 and 282 nm change in the same temperature range. On the other hand, the normalized CDs at 289 and 416 nm change in lower temperature range than that in which the CDs at 222 nm and 282 nm change. The mid-point temperature where the normalized CD becomes 0.5 at 222 nm, 282 nm, 289 nm, and 416 nm are 71.7 °C, 71.5 °C, 70.5 °C, and

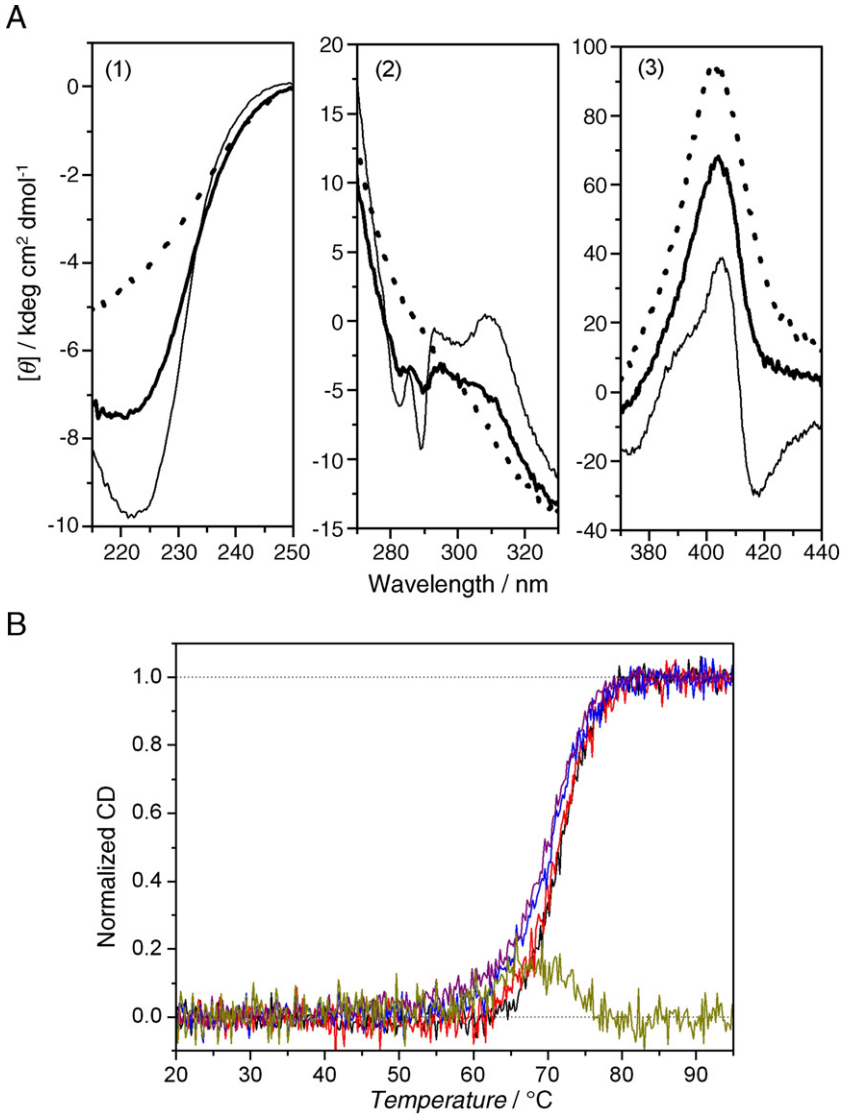

Fig. 6. (A) The CD spectra of Far-UV (1), Near-UV (2), and Soret regions(3) of horse cytochrome *c* at pH 4.1. The CD spectra of horse cytochrome *c* are observed at 20 °C (thin solid lines), 70 °C (thick solid lines), and 95 °C (dotted lines). (B) The temperature dependence of the normalized CD of several wavelengths, 222 nm (black line), 282 nm (red line), 289 nm (blue line), and 416 nm (purple line) on the thermal transition of cytochrome *c* at pH 4.1. The dark-yellow line shows the difference between normalized CDs induced by subtracting the normalized CD at 222 nm from that at 289 nm.

69.8 °C, respectively. The discrepancies in the mid-point temperature among the several wavelengths indicate the existence of at least one intermediate state in the thermal N–D transition of horse cytochrome *c*. The difference between normalized CDs–for example, subtracting the normalized CD at 222 nm from that at 289 nm–shows the largest value near 70 °C (Fig. 6B) where the mole fraction of the intermediate state determined by DSC becomes maximum (Fig. 3), indicating that the intermediate state detected by CD is the same state as that by DSC analysis.

In order to compare the CDs of these thermodynamic states, the normalized CDs of the intermediate state ($[\theta]_I^{nor}(T)$) at the four wave-lengths were evaluated by Eq. (15). All these functions were found to be well approximated as linear functions of temperature with slightly positive slopes. The values at 70 °C for 222 nm, 282 nm, 289 nm, and 416 nm were determined by linear least-squares fitting of these functions as 0.11, 0.22, 0.47, and 0.57, respectively.

4. Discussion

4.1. The intermediate state in the thermal transition of cytochrome c

Through precise DSC data and CD measurement, our study showed that the intermediate state exists in the thermal transition of horse cytochrome *c*. However, the thermal transition of cytochrome *c* has also been described with the two-state transition model by calorimetric and spectroscopic methods [20,23,30]. By virtue of the fact that Far-UV (222 nm) and near-UV (282 nm) CD were changed at the same temperature, the thermal transition of horse cytochrome *c* was

explained with the two-state transition by CD measurement [20]. Our study confirmed that the normalized CDs of cytochrome *c* at 289 and 416 nm are changed at lower temperatures than that at 222 nm (Fig. 6B). The discrepancies in the transition temperature among the several wavelengths indicates the existence of an intermediate state on the thermal N–D transition of horse cytochrome *c*.

In previous calorimetric studies, the heat capacity functions can be well explained by the two-state transition from the coincidence between ΔH^{cal} and ΔH^{vH} [23,30]. The small difference between these two enthalpies suggested an intermediate state populating around the transition temperature, although the fraction of the intermediate state was too small to be characterized quantitatively [23]. In our study, the mole fraction of the intermediate state is about 0.4 and the $\frac{\Delta H^{\mathrm{vH}}}{\Delta H^{\mathrm{cal}}}$ is 0.7 at around 70 °C, as evaluated by the DD method and the nonlinear least-squares fitting with the three-state model. These discrepancies in the fraction amount and in the value of $\frac{\Delta H^{\mathrm{vH}}}{\Delta H^{\mathrm{cal}}}$ are derived from the discrepancy between the baselines of the N and D states used for analyzing DSC curves. The ΔH_{ND} determined by the two-state analysis of our DSC data agrees with that of the previous report (Fig. 5), and the $\frac{\Delta H^{\mathrm{vH}}}{\Delta H^{\mathrm{cal}}}$ is 1.0. However, the fitting baselines determined by the two-state model deviated from the experimental data especially at the pre-transition temperature (Fig. 1B). On the other hand, the fitting base lines determined by the three-state model agree very well with the experimental heat capacity data. This discrepancy between the fitting baselines determined by the two-state model and the experimental heat capacity data can be evaluated in detail by using a highly precise differential scanning calorimeter, VP-DSC.

The $\Delta C_{\mathrm{p,\ NI}}$ was estimated at 0–3 kJ $\mathrm{K}^{-1}\mathrm{mol}^{-1}$, judging from the coincidence between the $\Delta C_{\mathrm{p,\ ND}}$ determined by the temperature dependence of ΔH_{ND} and the $\Delta C_{\mathrm{p,\ ND}}$ deduced from the three-state analysis of the single heat capacity profile. The results described up to now are almost unchanged when the $\Delta C_{\mathrm{p,\ NI}}$ is 0–3 kJ $\mathrm{K}^{-1}\mathrm{mol}^{-1}$.

In this study, the enthalpy change, ΔH_{ND}, of horse cytochrome *c* determined by the three-state transition model, is about 100 kJ mol^{-1} higher than that of ΔH_{ND} determined by the two-state transition model. By using the following equations, the Gibbs free-energy difference, ΔG_{ND}, is deduced from ΔH_{ND}.

$$\frac{\partial}{\partial T}\left(\frac{\Delta G}{T}\right) = \frac{\Delta H}{T^2} \tag{16}$$

The $\frac{\Delta G_{\mathrm{ND}}}{T}$ is largest when the temperature is −5 °C in the three-state transition model and 10 °C in the two-state transition model [30]. At temperature when the $\frac{\Delta G_{\mathrm{ND}}}{T}$ is largest, the mole fraction of the native state is largest. This indicates that the cold destabilization of horse cytochrome *c* is not generated above −5 °C at pH 4.1.

4.2. The molten globule-like intermediate state in a native condition

The normalized CD of the intermediate state ($[\theta]_{\mathrm{I}}^{\mathrm{nor}}$) of 222 nm, 282 nm, 289 nm, and 416 nm at 70 °C are 0.11, 0.22, 0.47, and 0.57, respectively. As the CD at 222 nm of the intermediate state is close to that of N state, the intermediate state was indicated to have a significant amount of native-like secondary structure. The $[\theta]_{\mathrm{I}}^{\mathrm{nor}}$ of 282 nm and 289 nm showed that the $[[\theta]_{\mathrm{I}}^{\mathrm{nor}}]$ at 282 nm and 289 nm of the intermediate state are rather near to N, but there are clear distinctions between that of N and intermediate state. It indicated that the specific side-chain packing of the tryptophane residue of the intermediate state remains, but the order of the structure is reduced than that of the N state. These properties of near-UV CD of the intermediate state are similar to that of MG state of cytochrome *c* previously reported. For example, the $[\theta]$ of near-UV CD of MG state is close to that of N state, and the $[\theta]$ at 282 nm is changed cooperatively in the thermal transition from MG to denatured state of cytochrome *c* [20].

4.3. Stability of the molten globule-like intermediate state of cytochrome c

4.3.1. Effect of the electrostatic repulsions on the stability of the molten globule state

The effect of the electrostatic repulsions on the stability of the MG state was evaluated by using acetylated horse cytochrome *c* with various degrees of charge repulsion [16]. At pH 1.8, the intact cytochrome *c* exists in the acid denaturation state. But the 16 acetylated cytochrome *c*, i.e., the 16 acetylated amino groups of cytochrome *c*, at pH 1.8 has a molten globule structure. The net charges of the intact and 16 acetylated horse cytochrome *c* at pH 1.8 are estimated to be +25 and +9, respectively. The MG state is stabilized by lowering the electrostatic repulsions of positive charge in acetylated cytochrome *c*. This stabilization mechanism can explain the stabilization of the MG state under low pH and high anion concentrations. The anions act to lower the electrostatic repulsions of positive charge.

In this study, the MG-like intermediate state of cytochrome *c* was observed under low anion concentrations at pH 4.1. The net charge of horse cytochrome *c* at this pH is estimated to be +18 based on the amino-acid composition and the intrinsic p*K*a of the residues. The reduction of the net positive charge number can be considered to be the main factor to stabilize the MG-like intermediate state at pH 4.1 even under low salt concentrations.

The 6 acetylated cytochrome *c* at pH 1.8 is estimated to have the same net charge as the intact molecule at pH 4. While almost all molecules of the 6 acetylated cytochrome *c* at 50 °C at pH 1.8 exist in the acid denatured state [16], the MG-like intermediate state is more stable than the denatured state at 50 °C at pH 4.1 (Fig. 3). This suggests that the electrostatic interaction caused between the negative charges of the deprotonated carboxyl groups at this pH and the positive charges in the intact molecule stabilize the MG-like intermediate state.

4.3.2. The enthalpy change and the heat capacity change in the thermal transition from molten globule to denatured state of cytochrome c

In this study, the $\Delta C_{\mathrm{p,NI}}$ is estimated to be 0–3 kJ $\mathrm{K}^{-1}\mathrm{mol}^{-1}$. Therefore, the $\Delta C_{\mathrm{p,MG-D}}$ is 3.2–6.2 kJ $\mathrm{K}^{-1}\mathrm{mol}^{-1}$ and the $\Delta H_{\mathrm{MG-D}}$ at 40 °C is 231–327 kJ mol^{-1}.

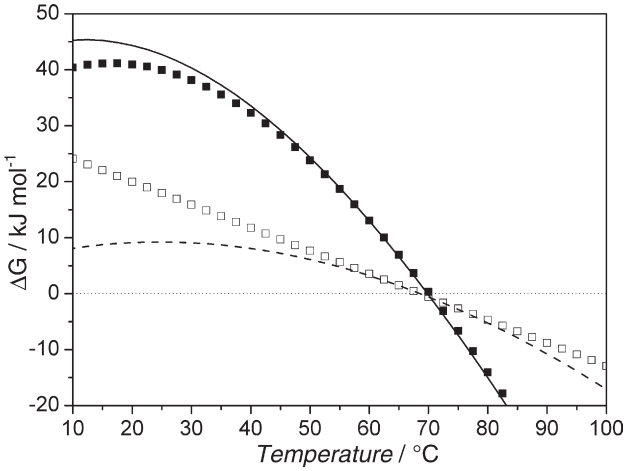

Fig. 7. The temperature dependence of the Gibbs free-energy change, ΔG. The filled squares show $\Delta G_{ND(0)}$ and the open squares show $\Delta G_{NI(0)}$, calculated with $\Delta C_{p,NI}$ fixed at 0 kJ $K^{-1}mol^{-1}$. The solid lines show $\Delta G_{ND(3)}$ and the broken lines show $\Delta G_{NI(3)}$, calculated with $\Delta C_{p,NI}$ fixed at 3 kJ $K^{-1}mol^{-1}$.

The $\Delta C_{p,MG-D}$ in this N–MG transition of bovine cytochrome *c* at pH 3.5 evaluated by IATC was 1.1 kJ $K^{-1}mol^{-1}$ [22]. This agrees with $\Delta C_{p,NI}$ in our study within error.

Potekhin et al. reported that the ΔH_{MG-D} at 40 °C and $\Delta C_{p,MG-D}$ are 160 kJ mol^{-1} and 0.65 kJ $K^{-1}mol^{-1}$, respectively, in the thermal transition of the MG state stabilized by chloride anion (Cl^-) at low pH, as determined by the two-state model [19]. Hamada et al. reported that the ΔH_{MG-D} at 40 °C and $\Delta C_{p,MG-D}$ are 131 kJ mol^{-1} and 1.5 kJ $K^{-1}mol^{-1}$, respectively, in the thermal transition of the MG state stabilized by perchlorate anion (ClO_4^-) at low pH, as determined by the two-state model from DSC measurements. In addition, they reported that the ΔH_{MG-D} at 40 °C and the $\Delta C_{p,MG-D}$ on the salt ($NaClO_4$)-induced transition from D to MG determined by the two-state model are 169.0 kJ mol^{-1} and 2.4 kJ $K^{-1}mol^{-1}$, respectively, from ITC measurements [21]. These values of the ΔH_{MG-D} and $\Delta C_{p,MG-D}$ are smaller than those estimated in our study. In another report, however, a CD study found that the thermal transition from the MG state stabilized by chlorate anion to the D state was not a two-state transition [20]. Therefore, the thermodynamic parameters determined by the two-state model should be reconsidered. Kuroda et al. reported that the ΔH_{MG-D} at 40 °C and $\Delta C_{p,MG-D}$ are 183 kJ mol^{-1} and 4.6 kJ $K^{-1}mol^{-1}$, respectively, in the thermal transition of the MG state stabilized by chloride anion (Cl^-) at low pH, as determined by the three-state model from CD measurements [20]. The $\Delta C_{p,MG-D}$ determined by CD by the three-state model agrees with the estimation in our study, within error.

4.3.3. The energetic properties of the molten globule-like intermediate state

Fig. 7 shows the temperature dependence of the Gibbs free-energy change, ΔG, on the transition from the N to the I and from the N to the D states. The $\Delta G_{ND(0)}$ mostly agrees with the $\Delta G_{ND(3)}$. On the other hand, the $\Delta G_{NI(0)}$ is different from the $\Delta G_{NI(3)}$, especially below 40 °C. The $\Delta G_{NI(0)}$ and $\Delta G_{ND(0)}$ are 22 kJ mol^{-1} and 41 kJ mol^{-1} at 15 °C. The $\Delta G_{NI(3)}$ and $\Delta G_{ND(3)}$ are 9 kJ mol^{-1} and 45 kJ mol^{-1} at 15 °C. The Gibbs free-energy change in the transition from the I to the D states, $\Delta G_{ID(0)}$ and $\Delta G_{ID(0)}$, are 19 kJ mol^{-1} and 36 kJ mol^{-1}, respectively, at 15 °C. The MG-like intermediate state in the thermal transition of horse cytochrome *c* under native conditions, such as pH 4.1 and low salt concentration, is more stable than the denatured state at 20 °C when the fixed $\Delta C_{p,NI}$ is 0–3 kJ $K^{-1}mol^{-1}$. Latypov et al. reported that ΔG_{NI} and ΔG_{ND} are 8.4 kJ mol^{-1} and 41.0 kJ mol^{-1} at 15 °C determined by the three-state analysis of the GuHCl-induced N–D transition of cytochrome *c* using spectroscopic method [33]. The ΔG_{NI} and ΔG_{ND} determined by the three-state analysis of the GuHCl-induced N–D transition of cytochrome *c* mostly agrees those in our study.

In this study, the free energy of the native state, the molten globule-like intermediate state, and the denatured state were evaluated under a native condition. The protein folding mechanism is understood the hierarchical folding funnel model is divided into two stages (1) stage I, formation of the molten globule state from the unfolded state with a large decrease in the conformational entropy; and (2) stage II, formation of the native state from the molten globule state [2]. Of course, for folding to proceed correctly, the MG state must have a lower energy level than the D state, and the N state must have a lower energy level than the MG state. The Gibbs free energies of the N, MG, and D states of cytochrome *c* evaluated in this study are consistent with the hierarchical folding funnel model. The structural study of the equilibrium MG state and the folding intermediate confirmed that the equilibrium MG state is identical to the transient intermediate state upon folding [2,4–6]. In this study, we have found the energetic implication that the equilibrium MG state is identical to the transient intermediate on folding.

References

[1] M. Ohgushi, A. Wada, 'Molten-globule state': a compact form of globular proteins with mobile side-chains, Febs Lett. 164 (1983) 21–24.
[2] M. Arai, K. Kuwajima, Role of the molten globule state in protein folding, Adv. Protein Chem. 53 (2000) 209–271.
[3] O.B. Ptitsyn, Molten globule and protein folding, Adv. Protein Chem. 47 (1995) 83–229.
[4] J. Balbach, V. Forge, W.S. Lau, N.A. Van Nuland, K. Brew, C.M. Dobson, Protein folding monitored at individual residues during a two-dimensional NMR experiment, Science 274 (1996) 1161–1163.
[5] W.C. Colon, G.A. Elove, P. Wakem, F. Sherman, H. Roder, Side chain packing of the N- and C-terminal helices plays a critical role in the kinetics of cytochrome *c* folding, Biochemistry 35 (1996) 5538–5549.
[6] W.C. Colon, H. Roder, Kinetic intermediates in the formation of the cytochrome *c* molten globule, Nat. Struct. Biol. 3 (1996) 1019–1025.
[7] G.W. Bushnell, G.V. Louie, G.D. Brayer, High-resolution three-dimensional structure of horse heart cytochrome *c*, J. Mol. Biol. 214 (1990) 585–595.
[8] M.F. Jeng, S.W. Englander, G.A. Elove, A.J. Wand, H. Roder, Structural description of acid-denatured cytochrome *c* by hydrogen exchange and 2D NMR, Biochemistry 29 (1990) 10433–10437.
[9] R. Santucci, C. Bongiovanni, G. Mei, T. Ferri, F. Polizio, A. Desideri, Anion size modulates the structure of the A state of cytochrome *c*, Biochemistry 39 (2000) 12632–12638.

[10] Y. Bai, T.R. Sosnick, L. Mayne, S.W. Englander, Protein folding intermediates: native-state hydrogen exchange, Science 269 (1995) 192–197.
[11] T. Ferri, A. Poscia, F. Ascoli, R. Santucci, Direct electrochemical evidence for an equilibrium intermediate in the guanidine-induced unfolding of cytochrome *c*, Biochim. Biophys. Acta 1298 (1996) 102–108.
[12] Y.G. Thomas, R.A. Goldbeck, D.S. Kliger, Characterization of equilibrium intermediates in denaturant-induced unfolding of ferrous and ferric cytochromes *c* using magnetic circular dichroism, circular dichroism, and optical absorption spectroscopies, Biopolymers 57 (2000) 29–36.
[13] Y.O. Kamatari, T. Konno, M. Kataoka, K. Akasaka, The methanol-induced globular and expanded denatured states of cytochrome *c*: a study by CD, Fluorescence, NMR and small-angle X-ray scattering, J. Mol. Biol. 259 (1996) 512–523.
[14] K. Chattopadhyay, S. Mazumdar, Stabilization of partially folded states of cytochrome *c* in aqueous surfactant: effects of ionic and hydrophobic interactions, Biochemistry 42 (2003) 14606–14613.
[15] S.H. Qureshi, B. Moza, S. Yadav, F. Ahmad, Conformational and thermodynamic characterization of the molten globule state occurring during unfolding of cytochromes-*c* by weak salt denaturants, Biochemistry 42 (2003) 1684–1695.
[16] Y. Goto, S. Nishikiori, Role of electrostatic repulsion in the acidic molten globule of cytochrome *c*, J. Mol. Biol. 222 (1991) 679–686.
[17] F. Sinibaldi, M.C. Piro, B.D. Howes, G. Smulevich, F. Ascoli, R. Santucci, Rupture of the hydrogen bond linking two Omega-loops induces the molten globule state at neutral pH in cytochrome *c*, Biochemistry 42 (2003) 7604–7610.
[18] M. Kataoka, Y. Hagihara, K. Mihara, Y. Goto, Molten globule of cytochrome *c* studied by small angle X-ray scattering, J. Mol. Biol. 229 (1993) 591–596.
[19] S. Potekhin, W. Pfeil, Microcalorimetric studies of conformational transition of ferricytochrome *c* in acidic solution, Biophys. Chemist. 34 (1989) 55–62.
[20] Y. Kuroda, S. Kidokoro, A. Wada, Thermodynamic characterization of cytochrome *c* at low pH. Observation of the molten globule state and of the cold denaturation process, J. Mol. Biol. 223 (1992) 1139–1153.
[21] D. Hamada, S. Kidokoro, H. Fukada, K. Takahashi, Y. Goto, Salt-induced formation of the molten globule state of cytochrome *c* studied by isothermal titration calorimetry, Proc. Natl. Acad. Sci. U. S. A. 91 (1994) 10325–10329.
[22] S. Nakamura, S. Kidokoro, Direct observation of the enthalpy change accompanying the native to molten-globule transition of cytochrome *c* by using isothermal acid-titration calorimetry, Biophys. Chemist. 113 (2005) 161–168.
[23] P.L. Privalov, N.N. Khechinashvili, A thermodynamic approach to problem of stabilization of globular protein structure, J. Mol. Biol. 86 (1974) 665–684.
[24] P.L. Privalov, Stability of proteins: small globular proteins, Adv. Protein Chem. 33 (1979) 167–241.
[25] G.I. Makhatadze, P.L. Privalov, Energetics of protein structure, Adv. Protein Chem. 47 (1995) 307–425.
[26] S. Kidokoro, A. Wada, Determination of thermodynamic functions from scanning calorimetry data, Biopolymers 26 (1987) 213–229.
[27] S. Kidokoro, A. Uedaira, A. Wada, Determination of thermodynamic functions from scanning calorimetry data II, Biopolymers 27 (1988) 271–297.
[28] T. Nakagawa, T. Oyanagi, in: Matushita (Ed.) (1980) Program system SALS for nonlinear least-squares fitting in experimental sciences, ed. Matushita, K. in Recent Developments in Statistical Inference and Data Analysis (North Holland Pub. Co. pp.221–225.
[29] S. Nakamura, S. Kidokoro, Isothermal acid-titration calorimetry for evaluating the pH dependence of protein stability, Biophys. Chemist. 109 (2004) 229–249.
[30] L. Fu, E. Freire, On the origin of the enthalpy and entropy convergence temperatures in protein folding, Proc. Natl. Acad. Sci. U. S. A. 89 (1992) 9335–9338.
[31] F. Sinibaldi, B.D. Howes, G. Smulevich, C. Ciaccio, M. Coletta, R. Santucci, Anion concentration modulates the conformation and stability of the molten globule of cytochrome *c*, J. Biol. Inorg. Chem. 8 (2003) 663–670.
[32] G.J. Pielak, K. Oikawa, A.G. Mauk, M. Smith, C.M. Kay, Elimination of the negative soret cotton effect of cytochrome *c* by replacement of the invariant phenylalanine, J. Am. Chem. Soc. 108 (1986) 2724–2727.
[33] R.F. Latypov, H. Cheng, N.A. Roder, J. Zhang, H. Roder, Structural characterization of an equilibrium unfolding intermediate in cytochrome *c*, J. Mol. Biol. 357 (2006) 1009–1025.